

1
2
3
4
5
6
7
8
9
10
11
12
13
14
15
16
17
18
19
20
21
22
23
24
25
26

Strain-level differences in gut microbiome composition determine fecal IgA levels and are modifiable by gut microbiota manipulation

Chao Yang^{1,2}, Ilaria Mogno^{1,2}, Eduardo J. Contijoch^{1,2}, Joshua N. Borgerding¹, Varun Aggarwala^{1,2}, Sophia Y. Siu², Zhihua Li², Emilie K. Grasset^{1,6}, Drew S. Helmus³, Marla C. Dubinsky³, Saurabh Mehandru¹, Andrea Cerutti^{1,4,5}, and Jeremiah J. Faith^{1,2,*}

¹Precision Immunology Institute, Icahn School of Medicine at Mount Sinai, New York, NY 10029, USA

²Icahn Institute for Data Science and Genomic Technology, Icahn School of Medicine at Mount Sinai, New York, NY 10029, USA

³Pediatric Gastroenterology and Hepatology, Department of Pediatrics, Susan and Leonard Feinberg IBD Clinical Center, Icahn School of Medicine at Mount Sinai, New York, NY 10029, USA

⁴Program for Inflammatory and Cardiovascular Disorders, Institut Hospital del Mar d'Investigacions Mediques (IMIM), Barcelona 08003, Spain

⁵Catalan Institute for Advanced Studies (ICREA), Barcelona 08003, Spain

⁶Department of Medicine, Center for Molecular Medicine, Karolinska Institutet, Karolinska University Hospital, SE-171 77 Stockholm, Sweden

*Correspondence: jeremiah.faith@mssm.edu (J.J.F.)

Keywords

Gut microbiota, Immunoglobulin A, *Bacteroides ovatus*, Fecal Microbiota Transplantation, Immune modulation

27 **Summary**

28 Fecal IgA production depends on colonization by a gut microbiota. However, the bacterial
29 strains that drive gut IgA production remain largely unknown. By accessing the IgA-inducing
30 capacity of a diverse set of human gut microbial strains, we identified *Bacteroides ovatus* as the
31 species that best induced gut IgA production. However, this induction varied bimodally across
32 different *B. ovatus* strains. The high IgA-inducing *B. ovatus* strains preferentially elicited more
33 IgA production in the large intestine largely through the T-cell-dependent B cell-activation
34 pathway. Remarkably, a low-IgA phenotype in mice could be robustly and consistently
35 converted into a high-IgA phenotype by transplanting a multiplex cocktail of high IgA-inducing *B.*
36 *ovatus* strains but not individual ones. Our results highlight the critical importance of microbial
37 strains in driving phenotype variation in the mucosal immune system and provide a strategy to
38 robustly modify a gut immune phenotype, including IgA production.

39

40 **Introduction**

41 Immunoglobulin A (IgA) is the most abundant mucosal antibody and plays an essential role in
42 maintaining gut homeostasis as well as other physiological processes (Cerutti and Rescigno,
43 2008; Macpherson et al., 2012; Sutherland et al., 2016). Secretory IgA, for example, can limit
44 the access of bacteria and bacteria-derived toxins to intestinal epithelial cells (Okai et al., 2016;
45 Tokuhara et al., 2010), facilitate the clearance of bacteria that have breached the mucosal
46 barrier (Fagarasan, 2008; Pabst, 2012; Strugnell and Wijburg, 2010) and regulate the
47 colonization of bacteria in the mucosal lining (Donaldson et al., 2018; McLoughlin et al., 2016).
48 In addition, IgA can also bind disease-associated gut microbiota (Kau et al., 2015; Palm et al.,
49 2014; Viladomiu et al., 2017). Conversely, the gut microbiota and its metabolites drive the
50 production of IgA as germ-free (GF) mice have an almost undetectable level of fecal IgA (Kim et
51 al., 2016; Macpherson et al., 2000). Upon bacteria colonization, even with a single bacterial
52 strain (Fritz et al., 2011; Hapfelmeier et al., 2010; Peterson et al., 2007), B cells undergo class-
53 switch to IgA⁺ cells in gut-associated lymphoid tissues (GALT), which include Peyer's patches
54 (PP), isolated lymphoid follicles (ILF) and mesenteric lymph nodes (MLN), and in the gut lamina
55 propria (LP) (Macpherson et al., 2008; Pabst, 2012). Much of the intestinal IgA is bacteria-
56 specific (Bunker et al., 2015; Hapfelmeier et al., 2010; Peterson et al., 2007), and the B-cell
57 repertoire is highly influenced by the microbiota composition (Lindner et al., 2015). To date, a
58 few murine derived bacterial species have been identified as being able to enhance or reduce
59 intestinal IgA level (Chudnovskiy et al., 2016; Lecuyer et al., 2014; Moon et al., 2015; Obata et
60 al., 2010). However, key questions regarding the impact of microbiota in this process remain
61 largely unanswered including the importance of colonization order, the contribution of individual
62 bacterial species versus that of microbial communities, the potential to modulate IgA production
63 by altering gut microbiota composition with commensal organisms, and the role of each
64 microbial species in the development of IgA⁺ B cells in specific tissues (Macpherson et al., 2015;
65 Pabst, 2012).

66 Apart from IgA-secreting cells, the gut microbiota has the capacity to influence numerous
67 other immune cell populations including colonic regulatory T cells (Treg) (Atarashi et al., 2011;
68 Faith et al., 2014; Round and Mazmanian, 2010), IL-17 producing T helper cells (Ivanov et al.,
69 2009), and macrophages (Mortha et al., 2014). Importantly, many of these responses seem to
70 be bacterial strain-specific as communities with comparable species composition can drive gut
71 immune responses characterized by largely different cell compositions (Britton et al., 2019).
72 These discoveries indicate that manipulation of the gut microbiota, with appropriate bacterial
73 strains, represents a potential therapeutic pathway for the treatment of diseases including
74 inflammatory bowel disease (IBD), rheumatoid arthritis (RA) and multiple sclerosis through
75 shaping the host immune system (Skelly et al., 2019) . Although the studies of microbiota-based
76 therapeutics and fecal microbiota transplantation (FMT) have heavily focused on the
77 engraftment of the transmitted microbiota and its influence on the composition of the recipient
78 microbiota (Seekatz et al., 2014; Shankar et al., 2014; Smillie et al., 2018), the clinical
79 application of microbiota manipulation as an immunomodulatory strategy will require
80 combinations of bacterial strains optimized for the induction of specific immune phenotypes that
81 are robust to the interpersonal variation in the pre-existing microbiota of each recipient.

82 Here we demonstrate that, upon transfer into GF mice, human isolates of the *Bacteroides*
83 *ovatus* species, one of the most common human gut commensals, are uniquely capable of
84 inducing high mucosal IgA production compared with other common gut commensal species.
85 This IgA-inducing capacity, however, was restricted to specific strains of *B. ovatus* that
86 preferentially led to IgA production in the large intestine through both T-cell-dependent (TD) and
87 T-cell-independent (TI) B cell-activation pathways. While no individual bacterial strain functioned
88 as an effective enhancer of gut IgA production, we found that cocktails of these high IgA-
89 inducing (IgA^{high}) strains could serve as effective immunomodulators, that elicited higher fecal
90 IgA levels upon administration to animals harboring a pre-existing microbiota with low IgA-
91 inducing potential (IgA^{low}). Our work demonstrates the importance of strain-level variation in gut

92 microbiota composition on mucosal immune responses. It also supports the potential utility of
93 cultured multi-bacterial effector strain cocktails as a strategy to overcome phenotype transfer
94 resistance in microbiota-based immunomodulation (Petrof and Khoruts, 2014).

95

96 **Results**

97 ***B. ovatus* elicits robust gut IgA production**

98 To determine if individual gut bacterial species have a distinct IgA-inducing potential, we
99 monocolonized GF C57BL/6 mice with one of eight different human gut commensal bacteria
100 (Table S1) with representatives from the most prominent phyla of the human gut including
101 Firmicutes, Bacteroidetes, Actinobacteria and Proteobacteria (Human Microbiome Project,
102 2012; Turnbaugh et al., 2009). After three weeks of colonization to allow optimal steady-state
103 gut IgA secretion (Figure S1A), we measured serum and fecal IgA levels in each group of
104 gnotobiotic mice (Peterson et al., 2007). Although all tested species significantly increased IgA
105 level relative to control GF mice, *B. ovatus* monocolonized mice secreted significantly more IgA
106 in their feces compared with mice colonized with any of the other seven human gut bacteria
107 (Figure 1A; $p < 0.001$). Most species also increased serum IgA (Figure S1B). However,
108 consistent with previous reports (Macpherson et al., 2008), fecal IgA and serum IgA levels in
109 these mice did not correlate significantly (Figure S1C; $R^2 = 0.226$; $p = 0.196$). GF mice colonized
110 with the cocktail of all eight bacterial species yielded as much fecal and serum IgA as mice
111 monocolonized with *B. ovatus*.

112 To address if the order of bacterial colonization could influence fecal IgA secretion, GF
113 mice were sequentially colonized every three weeks with individual species or small cocktails of
114 the same eight bacterial species. We first assayed fecal IgA level in mice sequentially colonized
115 with low IgA inducers (i.e. *E. coli*) to high IgA inducers (i.e. *B. ovatus*) (Figure S1D). Fecal IgA
116 increased gradually with the colonization of additional bacterial species. However, the more
117 striking (>2-fold) increase in IgA occurred after colonization with *B. ovatus* (Figure 1B).
118 Metagenomic sequencing of fecal microbiota in these mice revealed gut colonization by each
119 bacterial species, albeit with different proportions (Figure 1C). We then reversed the order of
120 colonization from high IgA inducers (i.e. *B. ovatus*) to low IgA inducers (i.e. *E. coli*) (Figure
121 S1D). Once again, *B. ovatus* elicited the largest increase of fecal IgA production, while the other

122 species led to smaller increases (Figure 1D). Remarkably, the relative abundance of each
123 organism at the end of the colonization was very similar, regardless of the order of colonization
124 (Figures 1C and 1E). These results demonstrate that *B. ovatus* is a uniquely potent gut IgA
125 inducer and that the species composition of the gut microbiota impacts IgA production more
126 than the order of bacterial colonization.

127 To test the role of bacterial viability in the induction of gut IgA by *B. ovatus* (Hapfelmeier et
128 al., 2010), GF mice were administered heat-killed *B. ovatus* or *B. ovatus* metabolites (i.e.
129 filtered, conditioned growth medium from stationary phase of *B. ovatus* cultures) for three
130 weeks. Neither approach was capable of enhancing fecal IgA above the level detected in GF
131 mice (Figure S1E). To ensure the above result was not due to the underdeveloped mucosal
132 immune system of GF mice, we performed similar experiments by first colonizing GF mice with
133 *E. coli* for three weeks and subsequently treated these mice with heat-killed *B. ovatus* for an
134 additional three weeks. Again, we found no significant fecal IgA increase (Figure S1E). Thus,
135 neither dead *B. ovatus* nor its metabolites triggered efficient gut IgA responses in the murine
136 intestine. All together, live *B. ovatus* species elicited more gut IgA production than other tested
137 gut commensal bacterial species in GF mice.

138

139 ***B. ovatus*-driven gut IgA production is strain-specific**

140 Given the remarkable microbial strain variation across individuals (Faith et al., 2015; Faith et al.,
141 2013; Vatanen et al., 2018; Zhao et al., 2019), we wondered whether all *B. ovatus* strains within
142 this common bacterial species induced comparably high fecal IgA. GF mice monocolonized for
143 three weeks with one of 19 *B. ovatus* strains isolated from 19 different individuals (Table S2)
144 showed a strain-specific gut IgA response (Figure 1F; $p < 0.0001$). In contrast to the large
145 variability of fecal IgA levels, serum IgA levels were comparable across mice monocolonized
146 with different *B. ovatus* strains (Figure S2A). Similarly, the colonization density was also
147 comparable across mice harboring different *B. ovatus* strains (Figure S2B). This observation

148 suggests that the global density of each individual strain was not implicated in the genesis of
149 strain-specific differences of gut IgA responses. Of note, the distribution pattern of IgA induction
150 across multiple *B. ovatus* strains was bimodal (Figure S2C; $p = 0.0481$ Hartigans' Dip Test),
151 allowing these strains to be categorized as IgA^{high} or IgA^{low}. The genomic similarity of *B. ovatus*
152 strains was not a significant predictor of their IgA^{high} and IgA^{low} properties (Figure 1G and Table
153 S3), which suggests that their distinct IgA-inducing function is shared amongst the species
154 rather than representing an evolutionarily distinct group within the species.

155 To rule out a bias in our preliminary screen for IgA^{low} strains within the *Bacteroides* genus,
156 we assayed whether additional strains could induce high fecal IgA (Figure 1A). We found no
157 strain-specific differences in fecal IgA induction when GF mice were monocolonized with three
158 distinct strains of *B. caccae*, *B. thetaiotaomicron* and *B. vulgatus* (Figure S2D). The IgA-
159 inducing function of additional common species from the order Bacteroidales, including
160 *Parabacteroides johnsonii*, *Bacteroides intestinalis* and *Bacteroides fragilis*, were tested but also
161 induced much less gut IgA than *B. ovatus* (Figure S2D). These results indicate that the high
162 IgA-inducing ability of *B. ovatus* is unique to this gut bacterial species and only to a subset of
163 strains.

164 To examine the influence of *B. ovatus* strain variation on host fecal IgA production in the
165 context of more complex gut microbiotas, we colonized GF mice with one of the seven
166 microbiota arrayed culture collections originally isolated from different human donors with each
167 collection consisting of 15-20 unique species (Britton et al., 2019). The arrayed culture
168 collections were assembled to reconstitute a donor microbiota each containing a unique *B.*
169 *ovatus* strain, which was already functionally tested by earlier monocolonization (Figure 1F). We
170 observed a significant positive correlation between the fecal IgA concentrations induced by an
171 individual *B. ovatus* strain and the fecal IgA concentrations elicited by a culture collection
172 representing the entire *B. ovatus*-containing microbiota from the same donor (Figures 1H and
173 S2E; $R^2 = 0.859$, $p = 0.0027$). Again, these results suggest that the *B. ovatus* strain composition

174 is a major contributor of gut IgA responses even when considered in the context of complex
175 microbial communities.

176 Unlike inbred laboratory mice housed in a highly controlled environment, human beings,
177 with different genetic background, are exposed to more complex continuum of factors including
178 some that were demonstrated to affect fecal IgA production such as genetics and diet (Fransen
179 et al., 2015; Kim et al., 2016). To determine whether *B. ovatus* could drive robust gut IgA
180 responses also in humans, we measured the fecal concentration of IgA in multiple human
181 donors and correlated this concentration with that of fecal IgA generated by GF mice
182 monocolonized with a *B. ovatus* strain isolated from identical donors. Though no significant
183 correlation was observed, there was a clear trend towards a positive correlation even in an
184 uncontrolled condition (Figures 1I and S2E; $R^2 = 0.2071$, $p = 0.0765$).

185 In total these results demonstrate that a subset of *B. ovatus* strains induce high fecal IgA
186 levels, which broadly influence the total fecal IgA output of the host even in the context of a
187 diverse gut microbiota.

188

189 **IgA^{high} *B. ovatus* strains induce more IgA production in the large intestine**

190 To interrogate the mechanisms underpinning gut IgA induction by different *B. ovatus* strains, GF
191 mice were colonized with a representative IgA^{high} or IgA^{low} strain (*B. ovatus* strain E and Q,
192 respectively). We quantified bacteria-bound IgA in the stool of mice. Monocolonization with the
193 IgA^{high} strain E not only induced more free fecal IgA but also more fecal bacteria-bound IgA than
194 the IgA^{low} strain Q (52.9% vs. 21.0% IgA-coated *B. ovatus*) (Figure 2A). In contrast, no
195 significant difference was observed in serum immunoglobulin isotypes (i.e. IgA, IgG1, IgG2a,
196 IgG2b, IgG3, IgM and IgE) in monocolonized mice harboring either *B. ovatus* strain E or Q
197 (Figures S2A and S3A).

198 Fecal IgA mostly derives from polymeric IgA released by IgA⁺ plasma cells residing in the
199 intestinal LP and translocated to the gut lumen across epithelial cells via transcytosis (Johansen

200 and Kaetzel, 2011). This process is mediated by a basolateral IgA (and IgM) transporter termed
201 polymeric immunoglobulin receptor (pIgR) (Johansen and Kaetzel, 2011). Independent groups
202 have reported that the expression of pIgR by gut epithelial cells is influenced by bacteria
203 stimulation both *in vivo* and *in vitro* (Hooper et al., 2001; Schneeman et al., 2005). To determine
204 if *B. ovatus* strain variation impacts fecal IgA level by modulating pIgR-mediated transcytosis,
205 we imaged the expression of pIgR by immunofluorescence staining in the small intestine and
206 the colon of mice colonized with either *B. ovatus* strain E (IgA^{high}) or Q (IgA^{low}). However, no
207 noticeable difference in protein expression or mRNA transcription of pIgR was observed
208 (Figures S3B and S3C). We also found that the two strains of *B. ovatus* colonized the colon
209 similarly without penetrating into epithelial cells and induced similar level of mRNA transcription
210 of Muc2 (Figures S3C and S3D). To further interrogate the mechanism underpinning the
211 increased fecal IgA in *B. ovatus* strain E colonized mice, we then quantified, by histology and
212 flow cytometry, IgA-secreting B cells in both small intestine and the colon. We found more IgA-
213 secreting B cells in the colonic LP of mice harboring *B. ovatus* strain E compared to mice
214 harboring strain Q, while no significant strain-specific difference was observed in the small
215 intestine (Figures 2B and 2C). Although PPs and MLNs usually serve as dominant IgA inductive
216 sites (Chorny et al., 2010; Fagarasan et al., 2010), we did not find a significant difference in IgA⁺
217 B cells induction at these sites by strain E or Q (Figures S4A and S4B).

218 Given the preferential expansion of IgA-secreting B cells in the colon of monocolonized
219 mice harboring *B. ovatus* strain E, we then explored whether luminal IgA levels would vary
220 between small and large intestinal regions. In the small intestine, we found that mice
221 monocolonized with *B. ovatus* strain E or Q had comparable luminal IgA levels (Figure 2D). In
222 contrast, mice monocolonized with strain E had significantly more luminal IgA from cecum to
223 distal colon than those colonized with strain Q (Figure 2D). Similar results were also observed
224 across all tested IgA^{high} and IgA^{low} *B. ovatus* strains (Figure S5). Thus, the IgA^{high} *B. ovatus*

225 strains induce more colonic IgA-secreting B cells compared to IgA^{low} *B. ovatus* strains, which
226 results in the secretion of more IgA to the large intestinal lumen.

227 To determine if these observations were unique to GF C57BL/6 mice, we recapitulated our
228 monocolonization strategy in GF Swiss Webster mice and found that fecal IgA was largely
229 comparable in gnotobiotic C57BL/6 and Swiss Webster mice colonized with identical bacterial
230 strains (Figures S6A-S6D; $R^2 = 0.601$, $p = 0.0011$). Moreover, IgA^{high} strain colonized gnotobiotic
231 Swiss Webster mice also secreted more intraluminal IgA in the large intestine compared with
232 IgA^{low} strain colonized mice (Figure S6E). Thus, bacteria-induced gut IgA production is similar
233 across different host genetic backgrounds.

234

235 ***B. ovatus* elicits gut IgA production primarily via TD B cell-activation pathway**

236 Gut IgA responses occur through TD and/or TI B cell-activation pathways (Fagarasan et al.,
237 2010). To determine the influence of CD4⁺ T cells on the gut IgA production induced by *B.*
238 *ovatus*, we depleted CD4⁺ T cells in mice by injecting with an anti-CD4 antibody five days prior
239 to and for three weeks after monocolonization with *B. ovatus* strain E or Q (Figures 3A and S7A-
240 S7C). On day seven post-colonization, fecal IgA increased in both T cell-depleted and T cell-
241 sufficient gnotobiotic mice, which suggests that CD4⁺ T cells are not a dominant factor in early
242 stage IgA induction. By day 14 post-colonization, control mice receiving an isotype-matched
243 irrelevant antibody generated significantly more fecal IgA than mice receiving anti-CD4 antibody
244 suggesting the majority of the steady state *B. ovatus* induced IgA is T cell dependent (Figure
245 3B). In addition to reduced free IgA, *B. ovatus*-bound IgA also decreased in the stool of CD4⁺ T
246 cell-depleted mice (Figure 3C) in both *B. ovatus* strain E or Q colonized mice. Moreover, in the
247 small intestine and the colon, the frequency of IgA-secreting B cells was reduced significantly
248 compared to that of IgA-secreting B cells being detected in the control CD4⁺ T cell-sufficient
249 mice (Figures 3D and S7D-S7G). In addition, these control mice showed more intraluminal IgA
250 than CD4⁺ T cell-depleted mice across the whole intestinal tract (Figure 3E).

251

252 **Multiplex cocktail of *B. ovatus* strains robustly modify gut IgA production**

253 Given the potential of gut microbiota manipulation as a therapeutic, we next determined whether
254 the high-IgA phenotype could be transferred to mice harboring microbiotas that induce a low
255 level of fecal IgA. For this purpose, we recolonized GF C57BL/6 mice with either *B. ovatus*
256 strain E (IgA^{high}) or Q (IgA^{low}) for three weeks, followed by cohousing these mice for an
257 additional three weeks (Figure 4A). After cohousing, mice monocolonized with *B. ovatus* strain
258 Q showed no significant change in fecal IgA. In contrast, mice colonized initially with *B. ovatus*
259 strain E had reduced fecal IgA, which raised the possibility that the low-IgA phenotype behaves
260 as a dominant character in the context of this simple bacterial community (Figure 4B).
261 Interestingly, the IgA^{low} *B. ovatus* strain Q also dominated the relative abundance of the
262 microbiota, as it represented ~95% of the microbiota compared with ~5% of *B. ovatus* strain E
263 (Figure 4C). In an attempt to overcome this resistance to transfer of the high-IgA phenotype to
264 mice with low-IgA phenotype, we performed a similar experiment but added three more IgA^{high}
265 *B. ovatus* strains. Under these conditions, the high-IgA phenotype was transferred to the
266 cohoused mice initially monocolonized with the IgA^{low} strain (Figure S8A). However, *B. ovatus*
267 strain Q still represented a substantial proportion (32.5 - 53.8%) of the relative abundance in this
268 bacterial community (Figure S8B). Thus, a multiplex cocktail of bacterial effector strains that
269 each individually can induce a specific phenotype provides a more robust strategy for
270 transferring a high-IgA phenotype.

271 Beyond cohousing, we further validated the above findings by transferring IgA^{high} strains by
272 oral gavage. Consistent with the cohousing results, mice first colonized with an IgA^{low} *B. ovatus*
273 strain and then given a defined microbial transplant (DMT) via oral gavage with an additional
274 IgA^{high} strain did not alter gut IgA secretion. In contrast, mice receiving a cocktail of four IgA^{high}
275 *B. ovatus* strains (*B. ovatus* 4M) produced significantly more fecal IgA (Figure 4D and Table
276 S4). Metagenomic sequencing results demonstrated that multiple *B. ovatus* strains colonized

277 the recipient mice (Figure 4E). Of note, IgA^{low} *B. ovatus* strain Q still dominated the relative
278 abundance of the gut microbiota in individual strain transfers (Figure 4E). IgA^{high} strains
279 accounted for 44% of the gut microbiota in the *B. ovatus* 4M DMT group with each individual
280 IgA^{high} strain having a distinct relative abundance (Figure 4E). Finally, we replicated these
281 results in mice pre-colonized with another IgA^{low} *B. ovatus* strain R (Figures S8C and S8D).

282 To validate these results in the setting of more complex gut microbiotas, we performed
283 similar experiments using either gnotobiotic mice pre-colonized by a synthetic cocktail of diverse
284 bacterial species that included *B. ovatus* IgA^{low} strain Q (Table S5) or gnotobiotic mice pre-
285 colonized with arrayed culture collections established from donors harboring a functionally
286 validated IgA^{low} *B. ovatus* strain (Figure 1H and Table S6). As with simpler communities,
287 transfer of the high-IgA phenotype was robustly achieved with *B. ovatus* 4M or a multiplex
288 cocktail of eight IgA^{high} *B. ovatus* strains (*B. ovatus* 8M) (Table S4) but not by individual IgA^{high}
289 *B. ovatus* strains (Figures 4F and S8E). Consistent with our previous findings, IgA was elevated
290 only in the large intestine (Figures 4G and S8F). The relative proportions of each IgA^{high} strain
291 and total relative abundance of all IgA^{high} strains in the stool of multiplex bacterial cocktail
292 recipient mice varied across recipient microbiota communities (Figures 4H, 4I, S8G and S8H).

293 Since *B. ovatus* strain C had a high relative abundance after DMT with *B. ovatus* 4M
294 across multiple recipient microbiotas, we examined whether this strain itself could convert low-
295 IgA producing mice to high-IgA producing mice. In recipient mice pre-colonized with either *B.*
296 *ovatus* strain Q or microbiota arrayed culture collection (i.e. HuLib1175B), transplantation of *B.*
297 *ovatus* strain C alone did not significantly increase fecal IgA on its own (Fig. 4d,f and
298 Supplementary Fig. 9a,b).

299 To further validate the IgA-inducing properties of our multiplex IgA^{high} *B. ovatus* cocktails,
300 we tested these cocktails in two additional gnotobiotic mouse models pre-colonized by human
301 microbiota arrayed culture collections with low-IgA potential (Table S6). Again, we found that the
302 multiplex IgA^{high} *B. ovatus* cocktails robustly increased fecal IgA (Figures S10A-S10F). Across

303 all of the tested *B. ovatus* 4M and *B. ovatus* 8M recipients, we did not find a correlation between
304 the total relative abundance of IgA^{high} strains and the fecal IgA levels, which indicates that
305 maximizing the total abundance of IgA^{high} *B. ovatus* strains does not necessarily increase gut
306 IgA production (Figure S10G-S10I). In summary, our results demonstrate that transfer of
307 multiplex IgA^{high} *B. ovatus* strain cocktails, but not that of individual IgA^{high} strains, consistently
308 and robustly modulates the immune system (e.g. IgA phenotype) across several complex pre-
309 existing gut microbiota.
310

311 Discussion

312 Functional differences of pathogenic bacteria at the strain level have been intensively studied in
313 the past decades and are a fundamental component of infectious disease clinical practice. More
314 recently the functional impact of bacterial strain variation is becoming apparent in the context of
315 the protective or disease-enhancing properties of the commensal microbiota (Arthur et al., 2012;
316 Britton et al., 2019; Palm et al., 2014; Palmela et al., 2018; Viladomiu et al., 2017). Here, we
317 identified that approximately half of the isolated strains from *B. ovatus* species, which is one of
318 the most common species of our gut commensal microbiota, drive increased IgA production in
319 the distal intestinal tract. Interestingly, we did not find that the variation in fecal IgA induced by
320 different *B. ovatus* strains was related to unique genetic lineages amongst strains or the density
321 of the bacteria in the feces. Through manipulation of the pre-existing gut microbiota
322 composition, we discovered that cocktails of IgA^{high} *B. ovatus* strains were more efficient than
323 individual IgA^{high} *B. ovatus* strains in converting mice with low gut IgA production into mice
324 producing large amounts of gut IgA.

325 IgA^{high} *B. ovatus* strains increased IgA production in distal but not proximal intestinal
326 segments by enhancing the ratio of IgA-secreting B cells. Remarkably, this induction was not
327 dominated by the migration of IgA⁺ B cells from canonical IgA inductive sites, as gnotobiotic
328 mice colonized with either IgA^{high} or IgA^{low} *B. ovatus* strains showed comparable IgA⁺ B cells in
329 PPs and MLNs. One possibility is that IgA^{high} *B. ovatus* strains locally elicit IgA production in the
330 large intestine including cecal patches, ILFs and LP (Cerutti and Rescigno, 2008; Fagarasan et
331 al., 2010; Masahata et al., 2014). Interestingly, mice harboring specific *B. ovatus* strains showed
332 no significant differences in the intestinal abundance of *B. ovatus*, which further highlights the
333 unique IgA-inducing properties of individual strains.

334 After IgA^{high} *B. ovatus* strain colonization, CD4⁺ T cell-depleted mice showed a reduced
335 ratio of IgA⁺ B cells in the gut, in turn leading to decreased luminal IgA significantly along the
336 entire intestinal tract. Of note, both CD4⁺ T cell-sufficient and T cell-depleted mice produced a

337 comparable level of gut IgA at the beginning post colonization, which suggests CD4⁺ T cells
338 play less of a role during the very early stage of IgA induction likely due to the dominance of the
339 TI B cell-activation pathway. Interestingly, a protein from the gut commensal *Lactobacillus*
340 *rhamnosus* was recently shown to locally elicit IgA production via gut epithelial cells (Wang et
341 al., 2017). Thus, further studies will be needed to delineate the precise mechanisms whereby
342 IgA^{high} *B. ovatus* strain colonized mice generate gut IgA. Nevertheless, our study highlights the
343 important contribution of CD4⁺ T cells in bacteria-mediated IgA production, especially in the
344 large intestine (Kawamoto et al., 2014; Kunisawa et al., 2013).

345 FMT has a high success rate in the treatment of recurrent *C. difficile* infection (van Nood et
346 al., 2013). However, its success in other indications, such as ulcerative colitis, is more limited
347 (Moayyedi et al., 2015; Rossen et al., 2015). Although improving bacteria engraftment remains
348 a key goal of microbiota manipulation (Grinspan and Kelly, 2015; Moayyedi et al., 2015; Rossen
349 et al., 2015), identifying new strategies that optimize the transfer of a specific immune
350 phenotype constitutes a goal with a potentially larger range of applications. Using IgA induction
351 as an example of immunomodulatory phenotype transfer, our data showed that multiplex
352 bacterial cocktails of IgA^{high} *B. ovatus* strains elicited a more robust phenotype transfer than any
353 individual strain, even in mice with complex gut ecosystem. This multiplex effector strain cocktail
354 strategy was robust across multiple recipients, pre-colonized with different low-IgA microbiotas,
355 and could represent an effective approach to modify gut immune parameters in addition to IgA.
356 Of note, across the tested inductions of IgA via gut microbiota manipulation with IgA^{high} *B.*
357 *ovatus* strains, we found that no single strain consistently dominated over the others. Thus,
358 multiplex bacterial cocktails do not appear to have “super strains” with dominant IgA-inducing
359 function. Rather, the combination of multiple IgA^{high} effector strains in these cocktails has an
360 IgA-inducing potential superior to that of any individual strain. Intriguingly, the relative
361 abundance of total *B. ovatus* species remained largely stable even after the introduction of one

362 to eight new strains suggesting that these new strains largely share the same ecological niches
363 as that occupied by the pre-existing *B. ovatus*.

364 Gut microbiota-based immunomodulation has shown great potential as a therapeutic in a
365 number of mouse models, including Treg induction to limit colitis (Atarashi et al., 2013),
366 mitigation of graft-versus-host disease (Mathewson et al., 2016), and alteration of immune
367 checkpoint inhibitor efficacy for immuno-oncology (Tanoue et al., 2019). As immunotherapeutic
368 bacterial cocktails move towards the clinic (Honda and Littman, 2016), a key factor in their
369 success will be robust and consistent manipulation of the desired immune populations. The
370 usage of multiplex cocktails with each strain independently capable of inducing the desired
371 immune modulation provides one potential route to a consistent immune response that is robust
372 to the variation in microbiome composition across individuals.

373 In summary, our results highlight the importance of bacterial strain variation on the IgA-
374 inducing potential of the gut microbiota. In addition, we also identify a new strategy (i.e.
375 multiplex bacterial strain cocktail) for the exploitation of strain variation in the development of
376 robust microbiota-based immunomodulation strategies.

377

378 **Methods**

379 **Mice**

380 Germ-free C57BL/6 and Swiss Webster mice were bred and maintained in flexible film
381 gnotobiotic isolators (Class Biologically Clean, Ltd.). All mice were group housed with a 12-hour
382 light/dark cycle and allowed *ad libitum* access to diet and water. All animal studies were carried
383 out in accordance with protocols approved by the Institutional Animal Care and Use Committee
384 (IACUC) in Icahn School of Medicine at Mount Sinai.

385

386 **Colonization of germ-free mice with cultured bacteria**

387 Germ-free mice (~8 weeks old) were colonized 200- μ l aliquot of bacteria suspension via oral
388 gavage. Colonized mice were housed in flexible film vinyl isolators or in filter top cages using
389 previously described techniques (Faith et al., 2013).

390

391 **Growth and isolation of bacterial strains**

392 All bacterial strains were obtained from previously banked stool, public culture repositories or
393 human gut microbiota arrayed culture collections (Faith et al., 2014). All bacterial strains
394 isolated for this study were isolated from deidentified stool samples from individuals under a
395 Mount Sinai IRB approved protocol (IRB-16-00008). All bacteria apart from *E. coli* were grown
396 under anaerobic condition at 37°C in Brain Heart Infusion medium supplemented with 0.5%
397 yeast extract (Difco Laboratories), 0.4% monosaccharide mixture, 0.3% disaccharide mixture, L-
398 cysteine (0.5 mg/ml; Sigma-Aldrich), malic acid (1 mg/ml; Sigma-Aldrich) and 5 μ g/ml hemin. *E.*
399 *coli* was cultured in LB Broth Miller (EMD Chemicals, Inc.) under aerobic condition at 37°C.

400

401 **Quantification of immunoglobulin A by ELISA**

402 Total fecal IgA were measured by sandwich ELISA. High-binding ELISA plates (Corning 3690)
403 were coated with 1 μ g/ml goat anti-mouse IgA (SouthernBiotech, AL) capture antibody overnight

404 at 4°C. Plates were washed and blocked with 1% BSA in PBS for 2 h at room temperature.
405 Diluted samples and standards were added and incubated overnight at 4°C. Captured IgA was
406 detected by horseradish peroxidase (HRP)-conjugated goat anti-mouse IgA antibody (Sigma-
407 Aldrich). ELISA plates were developed by TMB microwell peroxidase substrate (KPL, Inc.) and
408 quenched by 1 M H₂SO₄. Colorimetric reaction was measured at OD = 450 nm by a Synergy™
409 HTX Multi-Mode Microplate Reader (BioTek Instruments, Inc.). For the quantification of human
410 stool IgA, the same ELISA procedure as described above was performed except using anti-
411 human IgA and anti-human IgA-HRP antibodies (SouthernBiotech, AL). Corresponding
412 immunoglobulin isotypes were used as standards after serial dilutions.

413

414 **Detection of IgA-coated bacteria in feces**

415 IgA-coated fecal bacteria were measured by flow cytometry as previously described (Kau et al.,
416 2015; Palm et al., 2014). Briefly, mouse fecal pellets, stored at -80°C freezer after collection,
417 were dissolved in PBS to a final concentration of 100 milligram per milliliter PBS by weight,
418 thawed at room temperature, homogenized in vortex mixer and centrifuged at 4°C to remove
419 large particles. The supernatant was passed through a 40 µm sterile nylon filter and a small
420 aliquot of the bacteria suspension was collected for staining. Bacteria were pelleted by
421 centrifugation and washed in PBS/1%BSA/2mM EDTA buffer for 3 times. Non-specific binding
422 sites were first blocked with 50 µl 20% rat serum for 20 min at 4°C. Bacteria were then stained
423 with monoclonal rat anti-mouse IgA antibody (eBioscience, clone mA-6E1) for 30 min at 4°C.
424 After washing 3 times, bacterial pellets were resuspended in PBS containing SYBR Green I
425 (Invitrogen, USA). Samples were run through a BD LSR Fortessa™ cell analyzer and further
426 analyzed by FlowJo software (Tree Star, Inc.). Only SYBR positive events were regarded as
427 real bacteria and gated for further quantification of IgA-coated bacteria ([Figure S11A](#)).

428

429 **Lymphocyte isolation from tissues**

430 To isolate mononuclear cells from Peyer's patches (PPs), PPs were excised from mouse small
431 intestines and incubated in dissociation buffer, containing Hank's Balanced Salt Solution
432 (HBSS) without Ca^{2+} and Mg^{2+} (GIBCO), 10% fetal bovine serum (FBS), 5 mM EDTA and 15
433 mM HEPES, at 37°C for 30 min. Later, tissues were mechanically separated by pushing them
434 through a 70 μm strainer into Iscove's Modified Dulbecco's Medium (IMDM) supplemented with
435 2% FBS. Filtered cells were spun down, washed and resuspended in IMDM/2%FBS. Lamina
436 propria lymphocytes were isolated as described (Faith et al., 2014). Briefly, small intestines and
437 colons were excised, followed by removing visceral fat and intestinal contents. Tissues were
438 opened longitudinally, washed twice in HBSS and incubated in dissociation buffer for 30 min at
439 37°C with mild agitation to remove epithelium and intraepithelial lymphocytes. Tissues were
440 then washed three times in ice cold HBSS, cut into ~2 cm pieces and digested with collagenase
441 (Sigma-Aldrich), DNase I (Sigma-Aldrich) and dispase I (Corning). Cell suspensions were
442 filtered through 70 μm cell strainers, washed three times, and resuspended in IMDM/2%FBS.
443 Mesenteric lymph nodes were separated from mesenteric fat and dissociated in IMDM/2%FBS
444 by physically pressing the tissues between the frosted portions of two glass microscope slides.
445 The cell suspension was filtered through a 70 μm cell strainer, washed three times and
446 resuspended in IMDM/2%FBS.

447

448 **Flow cytometry analysis and antibodies**

449 Isolated mononuclear cells were washed in PBS and incubated with Zombie Aqua™ dye
450 (BioLegend) to distinguish live and dead cells. Before surface staining, non-specific binding of
451 immunoglobulin to Fc receptors was blocked by anti-mouse CD16/32 antibody (BD
452 Biosciences). Cells were stained in FACS buffer (PBS without $\text{Ca}^{2+}/\text{Mg}^{2+}$ supplemented with 2%
453 FBS and 2 mM EDTA) containing a mix of antibodies for 30 min at 4°C. The following antibodies
454 were purchased from BioLegend if not indicated otherwise: anti-mouse CD45 (clone 30-F11),
455 anti-mouse/human CD45R/B220 (clone RA3-6B2), anti-mouse GL7 (clone GL7), anti-mouse

456 CD4 (clones GK1.5 and RM4-4), anti-mouse IgA (eBioscience, clone mA-6E1). For the staining
457 of IgA⁺ cells, both surface and intracellular staining were performed. Multi-parameter analysis
458 was conducted with BD™ LSR II flow cytometry or BD LSR Fortessa™ cell analyzers and
459 analyzed with FlowJo software (Tree Star, Inc.). Only singlets and live cells were used in all
460 further analyses ([Figure S11B](#)).

461

462 **Immunofluorescence staining**

463 Immunofluorescence staining was performed as described previously (Moon et al., 2015).
464 Briefly, intestinal tissues were fixed in 10% neutral formalin overnight at 4°C, dehydrated in 15%
465 and 30% sucrose buffer sequentially and mounted in O.C.T Embedding Compound (Electron
466 Microscopy Sciences). Cryostat sections (~8 µm) were prepared, blocked with anti-CD16/32
467 antibody in 10% (v/v) rat serum/0.1% Triton-X100 in PBS for 30 min at room temperature and
468 incubated with the indicated primary antibodies at 4°C overnight. The following primary
469 antibodies were used: rat anti-mouse IgA-FITC (eBioscience, clone mA-6E1), goat anti-mouse
470 pIgR (R&D Systems, cat #: AF2800). Slides were washed in PBS for three times, incubated
471 with Alexa Fluor®-conjugated species-specific secondary antibody (Invitrogen) for 1 h at room
472 temperature if needed and finally mounted with ProLong® Gold Anti-fade Reagent with DAPI
473 (Invitrogen). Fluorescence images of sections were acquired with a LSM780 confocal laser-
474 scanning microscope (Carl Zeiss) and further processed in ImageJ if necessary.

475

476 **Depletion of CD4⁺ T cells in germ-free mice**

477 *In vivo* depletion of CD4⁺ T cells was performed as described (Kruisbeek, 2001). Briefly, germ-
478 free mice (8 weeks old) were first injected intraperitoneally (i.p.) with anti-mouse CD4
479 monoclonal antibody (Bio X Cell, clone GK1.5) or matched isotype control (Bio X Cell, clone
480 LTF-2) at 0.5 mg/day/mouse for 3 consecutive days. Five days after the first antibody injection,
481 mice were inoculated via oral gavage with *B. ovatus* strain E or Q. Then the injection was

482 performed every 3 days for a period of 3 weeks. Efficacy of T cell depletion in gnotobiotic mice
483 before and after *B. ovatus* colonization was evaluated by flow cytometry.

484

485 **Extraction of bacterial DNA from feces**

486 Each murine fecal pellet was collected into a 2 ml screw cap tube (Axygen Scientific,
487 SCT200SSC) and stored at -80°C freezer until processing. Each sample was mixed with 1.3 ml
488 of buffer, composed of 282 µl of DNA buffer A (20 mM Tris pH 8.0, 2 mM EDTA and 200 mM
489 NaCl), 200 µl of 20% SDS (v/w), 550 µl of Phenol:Chloroform:IAA (25:24:1) (Ambion, AM9732)
490 and 268 µl of Buffer PM (Qiagen, 19083), and 400 µl of 0.1 mm diameter zirconia/silica beads
491 (BioSpec, 11079101z). Next, the sample was mechanically lysed with a Mini-Beadbeater-96
492 (BioSpec, 1001) for 5 min at room temperature. After centrifuging for 5 min at 4000 rpm
493 (Eppendorf Centrifuge 5810 R), all aqueous phase was collected, mixed with 650 µl of Buffer
494 PM thoroughly before running through a Qiagen spin column. The column was washed twice
495 with Buffer PE (Qiagen, 19065). Attached DNA was eluted with 100 µl of Buffer EB (Qiagen,
496 19086) and quantified with Qubit™ dsDNA Assay Kit (Thermo Fisher Scientific,
497 Q32853/Q32854). Bacteria density was calculated by the following equation: Bacteria Density =
498 DNA yield per sample (ug) / weight of sample (mg) (Contijoch et al., 2019).

499

500 **Bacterial genome and metagenomic sequencing**

501 Purified bacterial template DNA (~250 ng) was sonicated and prepared using the NEBNext®
502 Ultra™ II DNA Library Prep kit. Samples were pooled and sequenced with an Illumina HiSeq
503 4000 with pair-end 150nt reads. Metagenomic sequencing reads were mapped back to the
504 reference genomes for each experiment to determine the relative abundance of each strain. To
505 uniquely distinguish each strain, 100K sequencing reads for each sample were mapped to the
506 unique regions of each genome and final abundances were scaled by the unique genome size
507 of each strain (i.e. genome equivalents), as previously described (McNulty et al., 2013).

508

509 **Statistical analysis**

510 Data are shown as mean \pm SEM. Statistical significance between two groups was assessed by
511 an unpaired, two-tailed Student's *t* test. Comparisons among three or more groups were
512 performed using One-way ANOVA. Bimodality distribution of IgA levels induced by different *B.*
513 *ovatus* strains was performed in R (R package 'diptest'). For correlation test, Pearson
514 correlation coefficient was employed. Data plotting, interpolation and statistical analysis were
515 performed using GraphPad Prism 6.0 (GraphPad Software, La Jolla, CA) or R statistical
516 software (version 3.2.2). A *p*-value less than 0.05 is considered statistically significant.

517

518 **Data and code availability**

519 Bacterial genomes and metagenomic sequencing reads for this study are available via NCBI
520 BioProject accession number PRJNA518912.

521

522 **Acknowledgments**

523 We are grateful to C. Fermin, E. Vazquez, and G. Escano for the husbandry of gnotobiotic mice;
524 Drs. Anuk A. Das, Dirk D. Gevers, Charlotte Cunningham-Rundles, Brian Brown and Thomas
525 Moran for helpful discussions and comments. This work was supported in part by the staff and
526 resources of the Gnotobiotic Mouse Core Facility, the Microbiome Translational Center, the
527 Flow Cytometry Core Facility, the Microscopy CoRE and the Scientific Computing Division in
528 Icahn School of Medicine at Mount Sinai. This work was supported by National Institutes of
529 Health Grants (NIGMS GM108505, NCCIH AT008661, NIDDK DK112978) and Janssen Human
530 Microbiome Institute (to J.J.F.) and NIH DK112679 (to E.J.C.).

531

532 **Author contributions**

533 C.Y. and J.J.F conceived the study and designed the experiments; C.Y., I.M., E.J.C., J.B., V.A.,
534 S.S., E.G., D.H., M.D. and J.J.F. collected samples and conducted the experiments; I.M. and
535 Z.L. provided bacterial isolates; C.Y., S.M., A.C. and J.J.F. analyzed data; C.Y. and J.J.F.
536 prepared the manuscript. All authors read and approved the final manuscript.

537

538 **Declaration of interests**

539 J.J.F. serves as a consultant for Janssen Research & Development LLC. The other authors
540 declare no conflict of interests.

541

542 References

- 543 Arthur, J.C., Perez-Chanona, E., Muhlbauer, M., Tomkovich, S., Uronis, J.M., Fan, T.J.,
544 Campbell, B.J., Abujamel, T., Dogan, B., Rogers, A.B., *et al.* (2012). Intestinal inflammation
545 targets cancer-inducing activity of the microbiota. *Science* 338, 120-123.
- 546 Atarashi, K., Tanoue, T., Oshima, K., Suda, W., Nagano, Y., Nishikawa, H., Fukuda, S., Saito,
547 T., Narushima, S., Hase, K., *et al.* (2013). Treg induction by a rationally selected mixture of
548 Clostridia strains from the human microbiota. *Nature* 500, 232-236.
- 549 Atarashi, K., Tanoue, T., Shima, T., Imaoka, A., Kuwahara, T., Momose, Y., Cheng, G.,
550 Yamasaki, S., Saito, T., Ohba, Y., *et al.* (2011). Induction of colonic regulatory T cells by
551 indigenous Clostridium species. *Science* 331, 337-341.
- 552 Britton, G.J., Contijoch, E.J., Mogno, I., Vennaro, O.H., Llewellyn, S.R., Ng, R., Li, Z., Mortha,
553 A., Merad, M., Das, A., *et al.* (2019). Microbiotas from Humans with Inflammatory Bowel
554 Disease Alter the Balance of Gut Th17 and RORgammat(+) Regulatory T Cells and Exacerbate
555 Colitis in Mice. *Immunity* 50, 212-224 e214.
- 556 Bunker, J.J., Flynn, T.M., Koval, J.C., Shaw, D.G., Meisel, M., McDonald, B.D., Ishizuka, I.E.,
557 Dent, A.L., Wilson, P.C., Jabri, B., *et al.* (2015). Innate and Adaptive Humoral Responses Coat
558 Distinct Commensal Bacteria with Immunoglobulin A. *Immunity* 43, 541-553.
- 559 Cerutti, A., and Rescigno, M. (2008). The biology of intestinal immunoglobulin A responses.
560 *Immunity* 28, 740-750.
- 561 Chorny, A., Puga, I., and Cerutti, A. (2010). Innate Signaling Networks in Mucosal IgA Class
562 Switching. *Adv Immunol* 107, 31-69.
- 563 Chudnovskiy, A., Mortha, A., Kana, V., Kennard, A., Ramirez, J.D., Rahman, A., Remark, R.,
564 Mogno, I., Ng, R., Gnjatic, S., *et al.* (2016). Host-Protozoan Interactions Protect from Mucosal
565 Infections through Activation of the Inflammasome. *Cell* 167, 444-456 e414.
- 566 Contijoch, E.J., Britton, G.J., Yang, C., Mogno, I., Li, Z., Ng, R., Llewellyn, S.R., Hira, S.,
567 Johnson, C., Rabinowitz, K.M., *et al.* (2019). Gut microbiota density influences host physiology
568 and is shaped by host and microbial factors. *Elife* 8.
- 569 Donaldson, G.P., Ladinsky, M.S., Yu, K.B., Sanders, J.G., Yoo, B.B., Chou, W.C., Conner,
570 M.E., Earl, A.M., Knight, R., Bjorkman, P.J., *et al.* (2018). Gut microbiota utilize immunoglobulin
571 A for mucosal colonization. *Science* 360, 795-800.
- 572 Fagarasan, S. (2008). Evolution, development, mechanism and function of IgA in the gut. *Curr*
573 *Opin Immunol* 20, 170-177.
- 574 Fagarasan, S., Kawamoto, S., Kanagawa, O., and Suzuki, K. (2010). Adaptive immune
575 regulation in the gut: T cell-dependent and T cell-independent IgA synthesis. *Annu Rev Immunol*
576 28, 243-273.
- 577 Faith, J.J., Ahern, P.P., Ridaura, V.K., Cheng, J., and Gordon, J.I. (2014). Identifying gut
578 microbe-host phenotype relationships using combinatorial communities in gnotobiotic mice. *Sci*
579 *Transl Med* 6, 220ra211.
- 580 Faith, J.J., Colombel, J.-F., and Gordon, J.I. (2015). Identifying strains that contribute to
581 complex diseases through the study of microbial inheritance. *Proceedings of the National*
582 *Academy of Sciences* 112, 633-640.
- 583 Faith, J.J., Guruge, J.L., Charbonneau, M., Subramanian, S., Seedorf, H., Goodman, A.L.,
584 Clemente, J.C., Knight, R., Heath, A.C., Leibel, R.L., *et al.* (2013). The long-term stability of the
585 human gut microbiota. *Science* 341, 1237-1243.
- 586 Fransen, F., Zagato, E., Mazzini, E., Fosso, B., Manzari, C., El Aidy, S., Chiavelli, A., D'Erchia,
587 A.M., Sethi, M.K., Pabst, O., *et al.* (2015). BALB/c and C57BL/6 Mice Differ in Polyreactive IgA
588 Abundance, which Impacts the Generation of Antigen-Specific IgA and Microbiota Diversity.
589 *Immunity* 43, 527-540.

590 Fritz, J.H., Rojas, O.L., Simard, N., McCarthy, D.D., Hapfelmeier, S., Rubino, S., Robertson,
591 S.J., Larijani, M., Gosselin, J., Ivanov, I., *et al.* (2011). Acquisition of a multifunctional IgA+
592 plasma cell phenotype in the gut. *Nature* 481, 199-203.

593 Grinspan, A.M., and Kelly, C.R. (2015). Fecal Microbiota Transplantation for Ulcerative Colitis:
594 Not Just Yet. *Gastroenterology* 149, 15-18.

595 Hapfelmeier, S., Lawson, M.A., Slack, E., Kirundi, J.K., Stoel, M., Heikenwalder, M., Cahenzli,
596 J., Velykoredko, Y., Balmer, M.L., Endt, K., *et al.* (2010). Reversible microbial colonization of
597 germ-free mice reveals the dynamics of IgA immune responses. *Science* 328, 1705-1709.

598 Honda, K., and Littman, D.R. (2016). The microbiota in adaptive immune homeostasis and
599 disease. *Nature* 535, 75-84.

600 Hooper, L.V., Wong, M.H., Thelin, A., Hansson, L., Falk, P.G., and Gordon, J.I. (2001).
601 Molecular analysis of commensal host-microbial relationships in the intestine. *Science* 291, 881-
602 884.

603 Human Microbiome Project, C. (2012). Structure, function and diversity of the healthy human
604 microbiome. *Nature* 486, 207-214.

605 Ivanov, I., Atarashi, K., Manel, N., Brodie, E.L., Shima, T., Karaoz, U., Wei, D., Goldfarb, K.C.,
606 Santee, C.A., Lynch, S.V., *et al.* (2009). Induction of intestinal Th17 cells by segmented
607 filamentous bacteria. *Cell* 139, 485-498.

608 Johansen, F.E., and Kaetzel, C.S. (2011). Regulation of the polymeric immunoglobulin receptor
609 and IgA transport: new advances in environmental factors that stimulate pIgR expression and its
610 role in mucosal immunity. *Mucosal Immunol* 4, 598-602.

611 Kau, A.L., Planer, J.D., Liu, J., Rao, S., Yatsunenkov, T., Trehan, I., Manary, M.J., Liu, T.C.,
612 Stappenbeck, T.S., Maleta, K.M., *et al.* (2015). Functional characterization of IgA-targeted
613 bacterial taxa from undernourished Malawian children that produce diet-dependent enteropathy.
614 *Sci Transl Med* 7, 276ra224.

615 Kawamoto, S., Maruya, M., Kato, L.M., Suda, W., Atarashi, K., Doi, Y., Tsutsui, Y., Qin, H.,
616 Honda, K., Okada, T., *et al.* (2014). Foxp3(+) T cells regulate immunoglobulin a selection and
617 facilitate diversification of bacterial species responsible for immune homeostasis. *Immunity* 41,
618 152-165.

619 Kim, M., Qie, Y., Park, J., and Kim, C.H. (2016). Gut Microbial Metabolites Fuel Host Antibody
620 Responses. *Cell Host Microbe* 20, 202-214.

621 Kruisbeek, A.M. (2001). In vivo depletion of CD4- and CD8-specific T cells. *Curr Protoc*
622 *Immunol Chapter 4*, Unit 4 1.

623 Kunisawa, J., Gohda, M., Hashimoto, E., Ishikawa, I., Higuchi, M., Suzuki, Y., Goto, Y., Panea,
624 C., Ivanov, I., Sumiya, R., *et al.* (2013). Microbe-dependent CD11b+ IgA+ plasma cells mediate
625 robust early-phase intestinal IgA responses in mice. *Nat Commun* 4, 1772.

626 Kunisawa, J., Kurashima, Y., Gohda, M., Higuchi, M., Ishikawa, I., Miura, F., Ogahara, I., and
627 Kiyono, H. (2007). Sphingosine 1-phosphate regulates peritoneal B-cell trafficking for
628 subsequent intestinal IgA production. *Blood* 109, 3749-3756.

629 Lecuyer, E., Rakotobe, S., Lengline-Garnier, H., Lebreton, C., Picard, M., Juste, C., Fritzen, R.,
630 Eberl, G., McCoy, K.D., Macpherson, A.J., *et al.* (2014). Segmented filamentous bacterium uses
631 secondary and tertiary lymphoid tissues to induce gut IgA and specific T helper 17 cell
632 responses. *Immunity* 40, 608-620.

633 Lindner, C., Thomsen, I., Wahl, B., Ugur, M., Sethi, M.K., Friedrichsen, M., Smoczek, A., Ott, S.,
634 Baumann, U., Suerbaum, S., *et al.* (2015). Diversification of memory B cells drives the
635 continuous adaptation of secretory antibodies to gut microbiota. *Nat Immunol* 16, 880-888.

636 Macpherson, A.J., Gatto, D., Sainsbury, E., Harriman, G.R., Hengartner, H., and Zinkernagel,
637 R.M. (2000). A primitive T cell-independent mechanism of intestinal mucosal IgA responses to
638 commensal bacteria. *Science* 288, 2222-+.

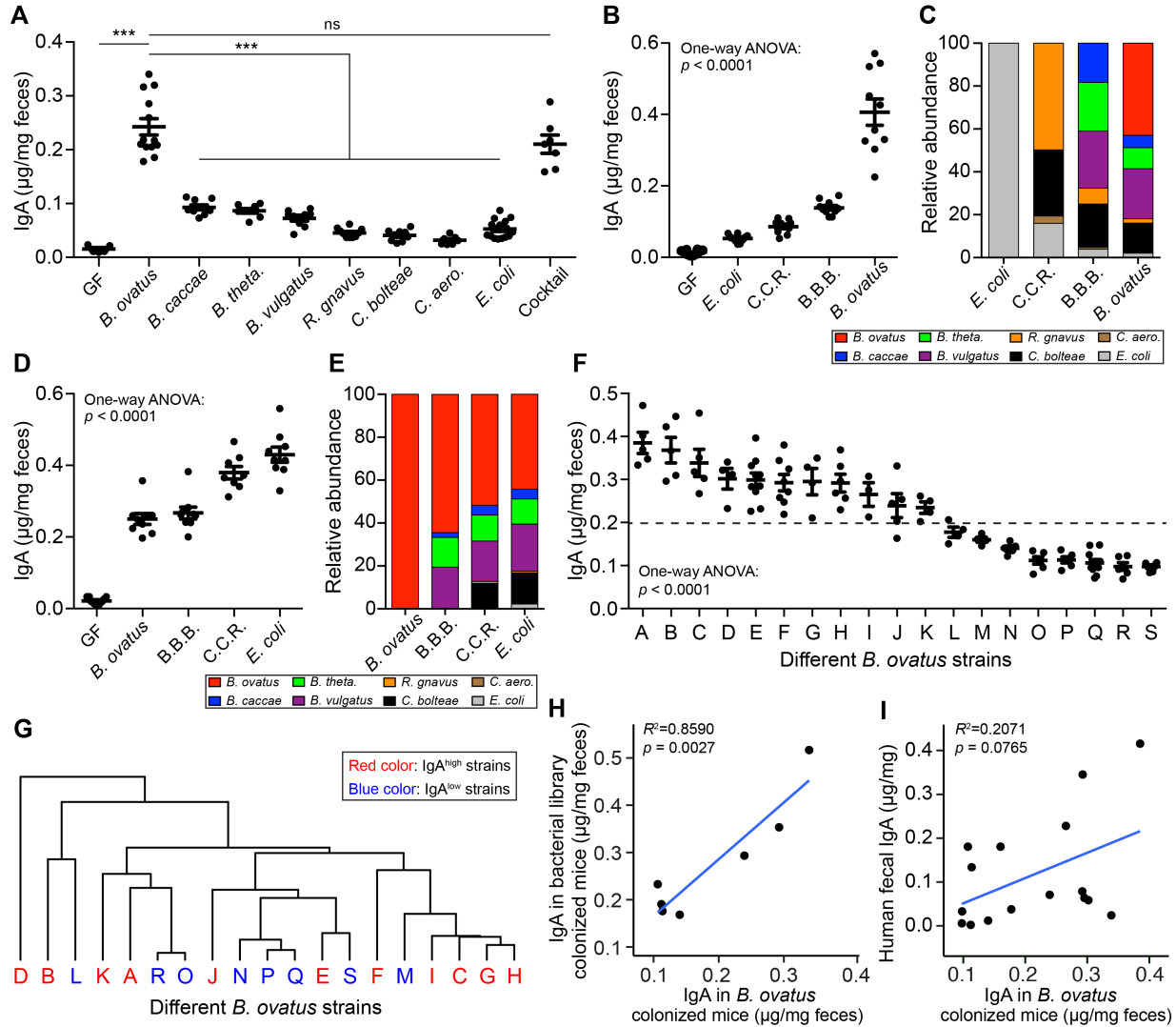
639 Macpherson, A.J., Geuking, M.B., and McCoy, K.D. (2012). Homeland Security: IgA immunity at
640 the frontiers of the body. *Trends Immunol* 33, 160-167.

- 641 Macpherson, A.J., Koller, Y., and McCoy, K.D. (2015). The bilateral responsiveness between
642 intestinal microbes and IgA. *Trends Immunol* 36, 460-470.
- 643 Macpherson, A.J., McCoy, K.D., Johansen, F.E., and Brandtzaeg, P. (2008). The immune
644 geography of IgA induction and function. *Mucosal Immunol* 1, 11-22.
- 645 Masahata, K., Umemoto, E., Kayama, H., Kotani, M., Nakamura, S., Kurakawa, T., Kikuta, J.,
646 Gotoh, K., Motooka, D., Sato, S., *et al.* (2014). Generation of colonic IgA-secreting cells in the
647 caecal patch. *Nat Commun* 5, 3704.
- 648 Mathewson, N.D., Jenq, R., Mathew, A.V., Koenigsnecht, M., Hanash, A., Toubai, T., Oravec-
649 Wilson, K., Wu, S.R., Sun, Y., Rossi, C., *et al.* (2016). Gut microbiome-derived metabolites
650 modulate intestinal epithelial cell damage and mitigate graft-versus-host disease. *Nat Immunol*
651 17, 505-513.
- 652 McLoughlin, K., Schluter, J., Rakoff-Nahoum, S., Smith, A.L., and Foster, K.R. (2016). Host
653 Selection of Microbiota via Differential Adhesion. *Cell Host Microbe* 19, 550-559.
- 654 McNulty, N.P., Wu, M., Erickson, A.R., Pan, C., Erickson, B.K., Martens, E.C., Pudlo, N.A.,
655 Muegge, B.D., Henrissat, B., Hettich, R.L., *et al.* (2013). Effects of diet on resource utilization by
656 a model human gut microbiota containing *Bacteroides cellulosilyticus* WH2, a symbiont with an
657 extensive glyco biome. *PLoS Biol* 11, e1001637.
- 658 Moayyedi, P., Surette, M.G., Kim, P.T., Libertucci, J., Wolfe, M., Onischi, C., Armstrong, D.,
659 Marshall, J.K., Kassam, Z., Reinisch, W., *et al.* (2015). Fecal Microbiota Transplantation
660 Induces Remission in Patients With Active Ulcerative Colitis in a Randomized Controlled Trial.
661 *Gastroenterology* 149, 102-+.
- 662 Moon, C., Baldrige, M.T., Wallace, M.A., D, C.A., Burnham, Virgin, H.W., and Stappenbeck,
663 T.S. (2015). Vertically transmitted faecal IgA levels determine extra-chromosomal phenotypic
664 variation. *Nature* 521, 90-93.
- 665 Mortha, A., Chudnovskiy, A., Hashimoto, D., Bogunovic, M., Spencer, S.P., Belkaid, Y., and
666 Merad, M. (2014). Microbiota-dependent crosstalk between macrophages and ILC3 promotes
667 intestinal homeostasis. *Science* 343, 1249288.
- 668 Nakamura, Y., Terahara, M., Iwamoto, T., Yamada, K., Asano, M., Kakuta, S., Iwakura, Y., and
669 Totsuka, M. (2012). Upregulation of Polymeric Immunoglobulin Receptor Expression by the
670 Heat-Inactivated Potential Probiotic *Bifidobacterium bifidum* OLB6378 in a Mouse Intestinal
671 Explant Model. *Scand J Immunol* 75, 176-183.
- 672 Obata, T., Goto, Y., Kunisawa, J., Sato, S., Sakamoto, M., Setoyama, H., Matsuki, T., Nonaka,
673 K., Shibata, N., Gohda, M., *et al.* (2010). Indigenous opportunistic bacteria inhabit mammalian
674 gut-associated lymphoid tissues and share a mucosal antibody-mediated symbiosis. *Proc Natl*
675 *Acad Sci U S A* 107, 7419-7424.
- 676 Okai, S., Usui, F., Yokota, S., Hori, I.Y., Hasegawa, M., Nakamura, T., Kurosawa, M., Okada,
677 S., Yamamoto, K., Nishiyama, E., *et al.* (2016). High-affinity monoclonal IgA regulates gut
678 microbiota and prevents colitis in mice. *Nat Microbiol* 1, 16103.
- 679 Pabst, O. (2012). New concepts in the generation and functions of IgA. *Nature Reviews*
680 *Immunology* 12, 821-832.
- 681 Palm, N.W., de Zoete, M.R., Cullen, T.W., Barry, N.A., Stefanowski, J., Hao, L., Degnan, P.H.,
682 Hu, J., Peter, I., Zhang, W., *et al.* (2014). Immunoglobulin A coating identifies colitogenic
683 bacteria in inflammatory bowel disease. *Cell* 158, 1000-1010.
- 684 Palmela, C., Chevarin, C., Xu, Z., Torres, J., Sevrin, G., Hirten, R., Barnich, N., Ng, S.C., and
685 Colombel, J.F. (2018). Adherent-invasive *Escherichia coli* in inflammatory bowel disease. *Gut*
686 67, 574-587.
- 687 Peterson, D.A., McNulty, N.P., Guruge, J.L., and Gordon, J.I. (2007). IgA response to symbiotic
688 bacteria as a mediator of gut homeostasis. *Cell Host Microbe* 2, 328-339.
- 689 Petrof, E.O., and Khoruts, A. (2014). From stool transplants to next-generation microbiota
690 therapeutics. *Gastroenterology* 146, 1573-1582.

691 Rossen, N.G., Fuentes, S., van der Spek, M.J., Tijssen, J.G., Hartman, J.H., Duflou, A.,
692 Lowenberg, M., van den Brink, G.R., Matus-Vliegen, E.M., de Vos, W.M., *et al.* (2015).
693 Findings From a Randomized Controlled Trial of Fecal Transplantation for Patients With
694 Ulcerative Colitis. *Gastroenterology* 149, 110-118 e114.
695 Round, J.L., and Mazmanian, S.K. (2010). Inducible Foxp3+ regulatory T-cell development by a
696 commensal bacterium of the intestinal microbiota. *Proc Natl Acad Sci U S A* 107, 12204-12209.
697 Ruane, D., Brane, L., Reis, B.S., Cheong, C., Poles, J., Do, Y., Zhu, H., Velinzon, K., Choi, J.H.,
698 Studt, N., *et al.* (2013). Lung dendritic cells induce migration of protective T cells to the
699 gastrointestinal tract. *J Exp Med* 210, 1871-1888.
700 Schneeman, T.A., Bruno, M.E.C., Schjerven, H., Johansen, F.-E., Chady, L., and Kaetzel, C.S.
701 (2005). Regulation of the Polymeric Ig Receptor by Signaling through TLRs 3 and 4: Linking
702 Innate and Adaptive Immune Responses. *The Journal of Immunology* 175, 376-384.
703 Seekatz, A.M., Aas, J., Gessert, C.E., Rubin, T.A., Saman, D.M., Bakken, J.S., and Young, V.B.
704 (2014). Recovery of the gut microbiome following fecal microbiota transplantation. *MBio* 5,
705 e00893-00814.
706 Shankar, V., Hamilton, M.J., Khoruts, A., Kilburn, A., Unno, T., Paliy, O., and Sadowsky, M.J.
707 (2014). Species and genus level resolution analysis of gut microbiota in *Clostridium difficile*
708 patients following fecal microbiota transplantation. *Microbiome* 2, 13.
709 Skelly, A.N., Sato, Y., Kearney, S., and Honda, K. (2019). Mining the microbiota for microbial
710 and metabolite-based immunotherapies. *Nat Rev Immunol* 19, 305-323.
711 Smillie, C.S., Sauk, J., Gevers, D., Friedman, J., Sung, J., Youngster, I., Hohmann, E.L., Staley,
712 C., Khoruts, A., Sadowsky, M.J., *et al.* (2018). Strain Tracking Reveals the Determinants of
713 Bacterial Engraftment in the Human Gut Following Fecal Microbiota Transplantation. *Cell Host*
714 *Microbe* 23, 229-240 e225.
715 Strugnell, R.A., and Wijnburg, O.L.C. (2010). The role of secretory antibodies in infection
716 immunity. *Nat Rev Microbiol* 8, 656-667.
717 Sutherland, D.B., Suzuki, K., and Fagarasan, S. (2016). Fostering of advanced mutualism with
718 gut microbiota by Immunoglobulin A. *Immunological Reviews* 270, 20-31.
719 Talham, G.L., Jiang, H.Q., Bos, N.A., and Cebra, J.J. (1999). Segmented filamentous bacteria
720 are potent stimuli of a physiologically normal state of the murine gut mucosal immune system.
721 *Infect Immun* 67, 1992-2000.
722 Tanoue, T., Morita, S., Plichta, D.R., Skelly, A.N., Suda, W., Sugiura, Y., Narushima, S.,
723 Vlamakis, H., Motoo, I., Sugita, K., *et al.* (2019). A defined commensal consortium elicits CD8 T
724 cells and anti-cancer immunity. *Nature* 565, 600-605.
725 Tokuhara, D., Yuki, Y., Nochi, T., Kodama, T., Mejima, M., Kurokawa, S., Takahashi, Y., Nanno,
726 M., Nakanishi, U., Takaiwa, F., *et al.* (2010). Secretory IgA-mediated protection against *V.*
727 *cholerae* and heat-labile enterotoxin-producing enterotoxigenic *Escherichia coli* by rice-based
728 vaccine. *Proc Natl Acad Sci U S A* 107, 8794-8799.
729 Turnbaugh, P.J., Hamady, M., Yatsunencko, T., Cantarel, B.L., Duncan, A., Ley, R.E., Sogin,
730 M.L., Jones, W.J., Roe, B.A., Affourtit, J.P., *et al.* (2009). A core gut microbiome in obese and
731 lean twins. *Nature* 457, 480-484.
732 van Nood, E., Vrieze, A., Nieuwdorp, M., Fuentes, S., Zoetendal, E.G., de Vos, W.M., Visser,
733 C.E., Kuijper, E.J., Bartelsman, J.F., Tijssen, J.G., *et al.* (2013). Duodenal infusion of donor
734 feces for recurrent *Clostridium difficile*. *N Engl J Med* 368, 407-415.
735 Vatanen, T., Plichta, D.R., Somani, J., Munch, P.C., Arthur, T.D., Hall, A.B., Rudolf, S., Oakeley,
736 E.J., Ke, X., Young, R.A., *et al.* (2018). Genomic variation and strain-specific functional
737 adaptation in the human gut microbiome during early life. *Nat Microbiol*.
738 Viladomiu, M., Kivolowitz, C., Abdulhamid, A., Dogan, B., Victorio, D., Castellanos, J.G., Woo,
739 V., Teng, F., Tran, N.L., Sczesnak, A., *et al.* (2017). IgA-coated *E. coli* enriched in Crohn's
740 disease spondyloarthritis promote TH17-dependent inflammation. *Sci Transl Med* 9.

741 Wang, Y., Liu, L., Moore, D.J., Shen, X., Peek, R.M., Acra, S.A., Li, H., Ren, X., Polk, D.B., and
742 Yan, F. (2017). An LGG-derived protein promotes IgA production through upregulation of APRIL
743 expression in intestinal epithelial cells. *Mucosal Immunol* 10, 373-384.
744 Wlodarska, M., Willing, B., Keeney, K.M., Menendez, A., Bergstrom, K.S., Gill, N., Russell, S.L.,
745 Vallance, B.A., and Finlay, B.B. (2011). Antibiotic Treatment Alters the Colonic Mucus Layer
746 and Predisposes the Host to Exacerbated *Citrobacter rodentium*-Induced Colitis.
747 *Infection and Immunity* 79, 1536-1545.
748 Zhao, S., Lieberman, T.D., Poyet, M., Kauffman, K.M., Gibbons, S.M., Groussin, M., Xavier,
749 R.J., and Alm, E.J. (2019). Adaptive Evolution within Gut Microbiomes of Healthy People. *Cell*
750 *Host Microbe* 25, 656-667 e658.
751

752 Figures and legends



753

754 **Figure 1. *B. ovatus* species, with strain-level differences, predominantly induces fecal**

755 **IgA production in gnotobiotic mice. (A) Fecal IgA level in C57BL/6 gnotobiotic mice**

756 **colonized with individual or a cocktail of human gut commensal bacteria for three weeks. (B-E)**

757 **The concentration of fecal IgA (B and D) and proportion of each bacterial strain (C and E) in**

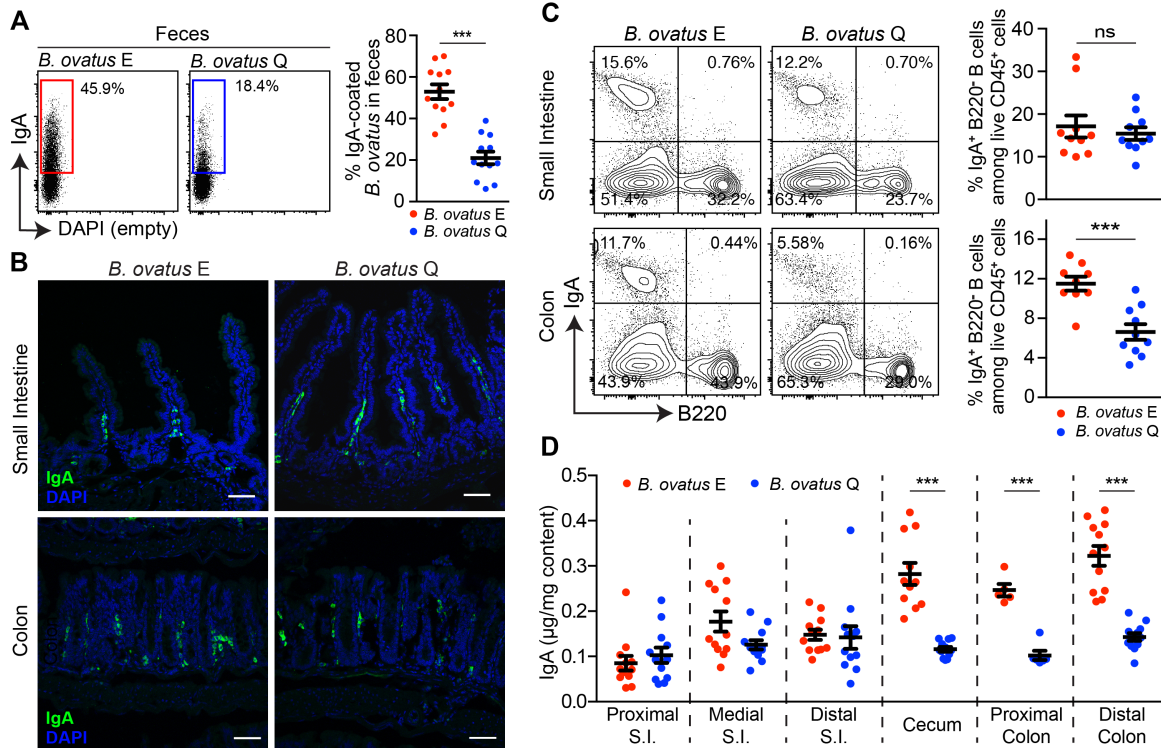
758 **stool of gnotobiotic mice that were colonized sequentially with individual or combined bacterial**

759 **communities starting from *E. coli* (B and C) or *B. ovatus* (D and E). Feces were harvested**

760 **before addition of new bacteria to the same mice. C.C.R.: cocktail of *C. bolteae*, *C. aerofaciens***

761 **and *R. gnavus*; B.B.B.: cocktail of *B. caccae*, *B. theta*. and *B. vulgatus* (F) Quantification of fecal**

762 IgA in gnotobiotic mice upon colonization with an individual strain of *B. ovatus* for three weeks.
763 Unique strains of *B. ovatus* were isolated from the stools of different human donors. Dotted line
764 separates high- and low-IgA phenotypes. (G) Dendrogram clustering of different *B. ovatus*
765 strains basing on the dissimilarity of bacterial genomic DNA sequences. (H) Correlation of stool
766 IgA levels between single *B. ovatus* strain monocolonized mice versus mice colonized with a
767 microbiota arrayed culture collection that included that single *B. ovatus* strain. Both single *B.*
768 *ovatus* strains and arrayed culture collections were isolated from the same donor. (i) Correlation
769 of fecal IgA concentration between single *B. ovatus* strain colonized mice versus human donor.
770 Data shown are mean \pm standard error of the mean. Each dot in **A**, **B**, **D** and **F** represents a
771 biological replicate. The average fecal IgA concentration from 4-10 mice was used for
772 correlation in **H** and **I**. Detailed strain information is listed in [Tables S1 and S2](#). p -values with
773 statistical significance (assessed by two-tailed Student's t test or one-way ANOVA) are
774 indicated: *** $p < 0.001$; ns, not significant.
775



776

777 **Figure 2. IgA^{high} *B. ovatus* strain Elicits stronger IgA responses in the large intestine. (A)**

778 Representative flow cytometry plot and quantification of IgA-coated *B. ovatus* in feces of

779 gnotobiotic mice harboring either *B. ovatus* strain E or Q. (B) Representative images of IgA⁺

780 cells in small intestine and the colon are shown. IgA⁺ cells were stained with anti-IgA (green);

781 Nuclei were counter-stained with DAPI (4',6-diamidino-2-phenylindole) (blue). n = 5~6. Scale

782 bar = 50 μm. (C) Percentage of IgA⁺ B cells, analyzed by flow cytometry, in small intestine and

783 colon is shown. Number adjacent to gate represents percentage. (D) Free IgA concentration in

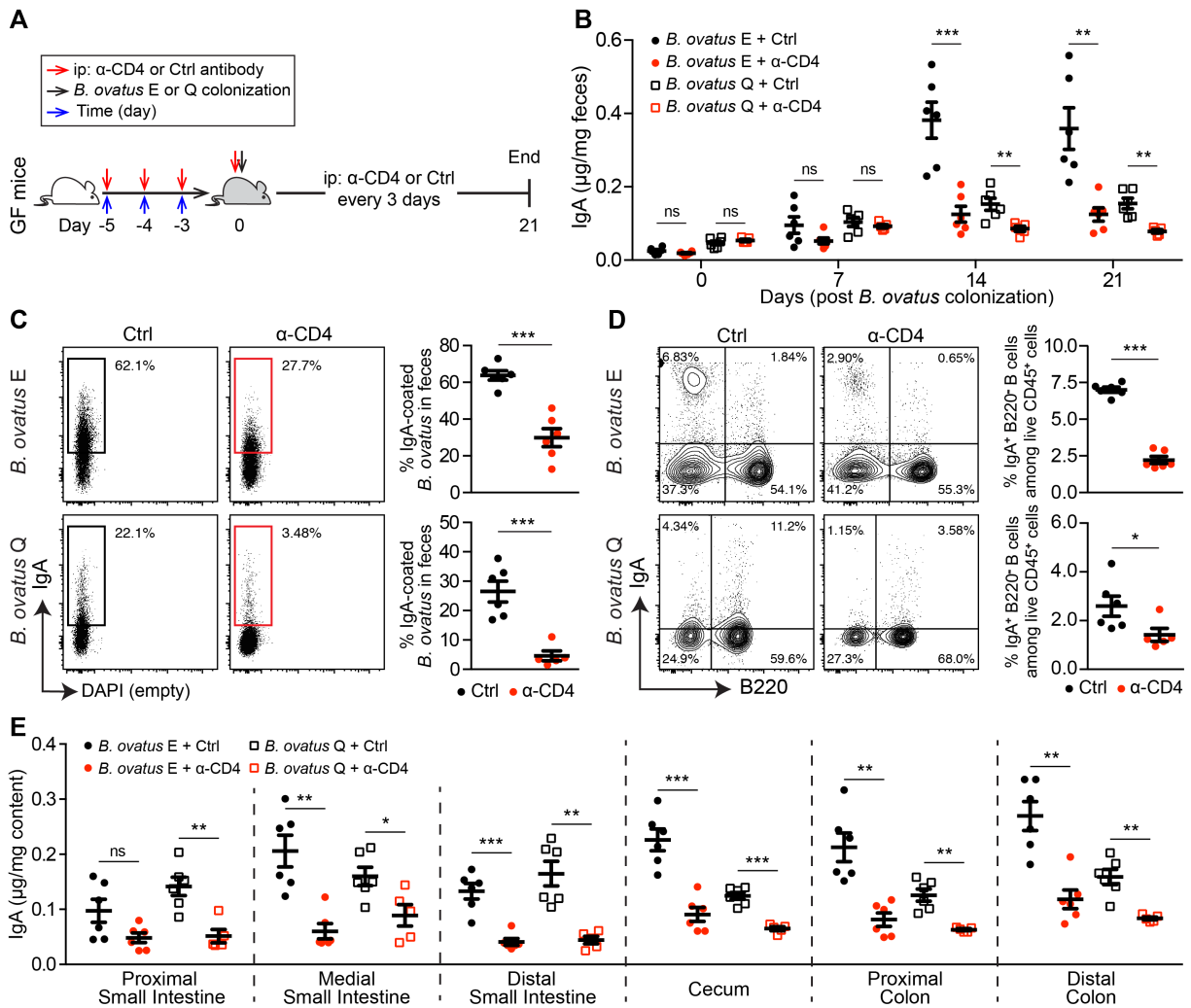
784 luminal contents along the length of the intestine. S.I.: small intestine. Data shown are mean ±

785 standard error of the mean. Each dot represents an individual mouse. *p*-values with statistical

786 significance (assessed by two-tailed Student's *t* test) are indicated: ****p* < 0.001; ns, not

787 significant.

788



789

790 **Figure 3. T-cell-dependent B cell activation pathway plays an essential role in *B. ovatus***

791 **induced fecal IgA production.** (A) Schematic representation of CD4⁺ T cells depletion in

792 germ-free B6 mice is illustrated. Red arrows represent i.p. injection of anti-CD4 antibody or

793 isotype control. Black arrow indicates *B. ovatus* strain E or Q colonization and blue arrows

794 represent time. (B) Dynamics of fecal IgA concentration in *B. ovatus* strain E or Q colonized

795 gnotobiotic B6 mice treated with either anti-CD4 antibody or isotype control. (C) Representative

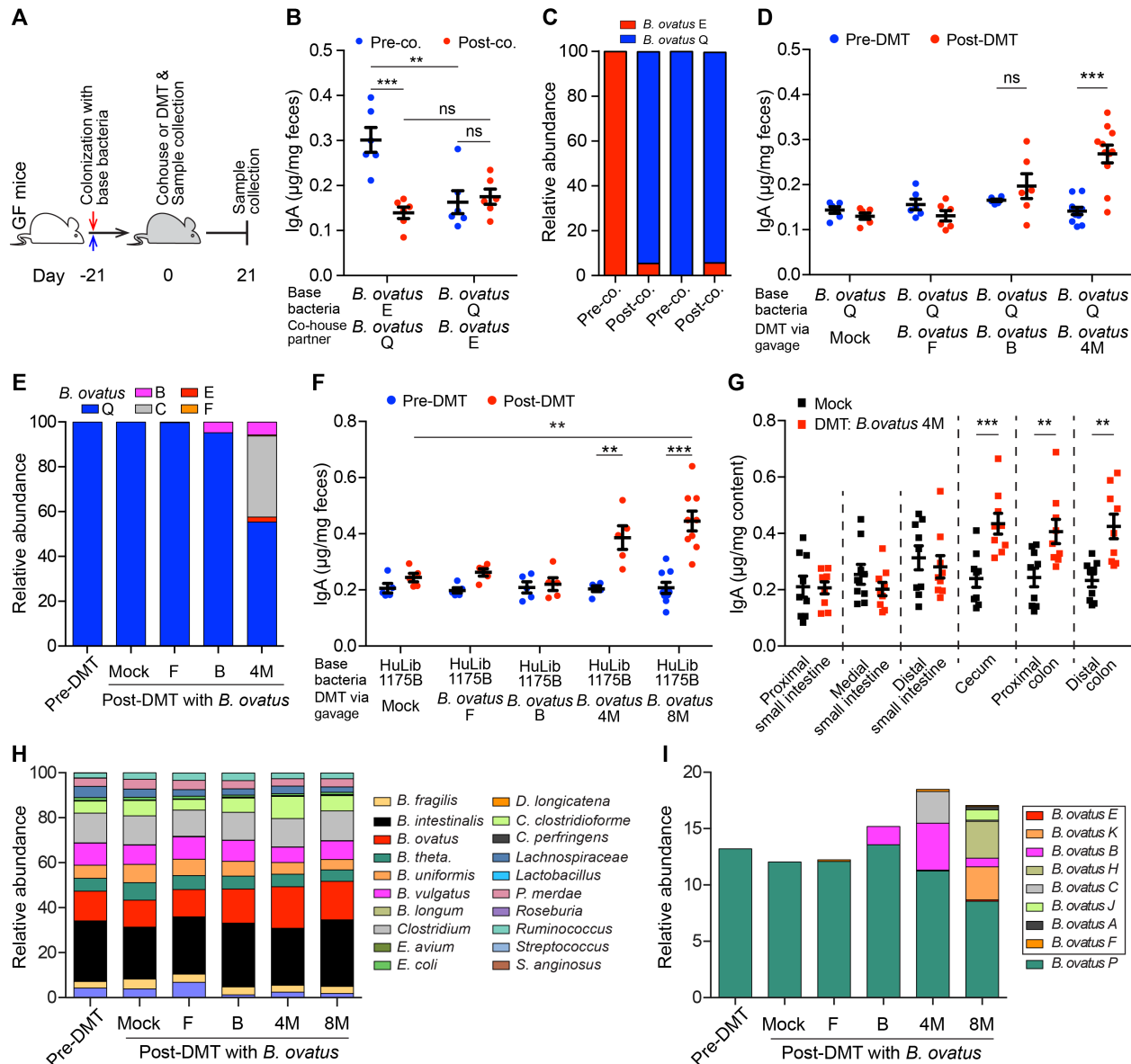
796 flow cytometry plot and quantification of IgA-coated bacteria in feces of *B. ovatus* strain E or Q

797 colonized gnotobiotic mice treated with either anti-CD4 antibody or isotype control. (D)

798 Representative flow cytometry plot and percentage of IgA-secreting B cells in the colon of mice

799 colonized with *B. ovatus* strain E or Q w/o anti-CD4 antibody treatment are shown. Numbers

800 adjacent to gates represent percentage. **(E)** Concentration of free IgA in the intestinal content
801 collected from different regions of the whole intestinal tract is shown. Data shown are mean \pm
802 standard error of the mean. Each dot represents an individual mouse. p -values with statistical
803 significance (assessed by two-tailed Student's t test) are indicated: * $p < 0.05$, ** $p < 0.01$, *** $p <$
804 0.001; ns, not significant.
805



806

807 **Figure 4. Multiplex microbial strains robustly transfer high-IgA phenotype to low-IgA**

808 **producing mice. (A)** Schematic representation of cohousing and defined microbial transplant

809 **(DMT) strategies. (B and C)** Fecal IgA concentration **(D)** and relative abundance of each *B.*

810 *ovatus* strain **(E)** in pre- and post-cohoused gnotobiotic mice, which were pre-colonized with

811 either *B. ovatus* strain E or Q. **(D and E)** Fecal IgA concentration **(D)** and relative abundance of

812 each *B. ovatus* strain **(E)** in mice pre- and post-microbial transplantation. Mice were first

813 colonized with *B. ovatus* strain Q for three weeks and subsequently administered cultured

814 microbes comprised of either an individual IgA^{high} *B. ovatus* strain or a cocktail of IgA^{high} *B.*

815 *ovatus* strains. (F) Fecal IgA concentration in mice pre- and post-DMT, which were pre-
816 colonized with human microbiota arrayed culture collection (i.e. HuLib1175B) for three weeks.
817 The administered microbes were either an individual IgA^{high} *B. ovatus* strain or a cocktail of
818 IgA^{high} *B. ovatus* strains. Mock: PBS; *B. ovatus* 4M: a cocktail of 4 different IgA^{high} *B. ovatus*
819 strains; *B. ovatus* 8M: a cocktail of 8 different IgA^{high} *B. ovatus* strains. (G) Free IgA
820 concentration along the intestinal tract of mice after DMT with Mock or *B. ovatus* 4M. (H)
821 Relative abundance of bacterial species in mice pre- and post-DMT. (I) Relative abundance of
822 different *B. ovatus* strains in mice pre- and post-DMT. Data shown are mean ± standard error of
823 the mean. Sequencing plots display the average relative abundance of bacteria from five mice.
824 Each dot represents a biological replicate. Detailed strain information is listed in [Tables S2 and](#)
825 [S6](#). *p*-values with statistical significance (assessed by two-tailed Student's *t* test) are indicated:
826 **p* < 0.05, ***p* < 0.01, ****p* < 0.001; ns, not significant.

827